

Linear undulator brightness: Inclusion of sextupolar magnetic-field contributions and of higher-order energy corrections

G. Dattoli, L. Giannessi, L. Mezi, M. Richetta, and A. Torre

*Ente per le Nuove Tecnologie, l'Energia e l'Ambiente, Area INN, Dipartimento Sviluppo Tecnologie di Punta,
P.O. Box 65, 00044 Frascati, Rome, Italy*

(Received 24 June 1991; revised manuscript received 10 October 1991)

In this paper we discuss the theory of emission by relativistic electrons in linearly polarized undulators. We show that the analytical computations are greatly simplified by the introduction of the so-called generalized Bessel functions, originally introduced to treat problems for which the dipolar approximation does not hold. We also discuss the modification induced in the brightness by the inclusion of the sextupolar terms, which arise when electrons are injected off the undulator axis. We show that the phenomenology inherent to this problem is very rich, as additional harmonics come into play and may cause sizable effects. The analysis we develop may be useful to obtain further insight in the physics underlying the so-called inhomogeneously broadened regime. Finally, we also discuss the inclusion of energy corrections up to $1/\gamma^3$ and the relevant physical consequences.

PACS number(s): 41.60.Ap, 41.60.Cr, 41.75.Ht, 52.75.Ms

I. INTRODUCTION

Synchrotron radiation, produced using undulators or wigglers, has been used, during recent years, as a powerful tool for many problems in pure and applied research [1]. These devices have been utilized as insertion elements on storage rings and, more recently, as an "active medium" for free-electron-laser experiments using low-energy accelerators.

An undulator can be exploited in a variety of ways and in fact its radiation may be the tool for a wide number of applications as, e.g., the diagnostics of the quality of the emitting beam or of the undulator itself [2]. At the same time the spectral features of the undulator radiation depend on a large number of effects. For this reason numerical codes, able to include the various aspects of an actual experimental configuration, have been developed during recent years. However, sometimes the codes, albeit very useful, may not allow a transparent understanding of the underlying physical problems.

We have stressed that undulator magnets have been used both on storage rings and on low-energy accelerators. Although the basic physical effects underlying the emission process are the same in both devices, obvious differences arise due to, e.g., the energies, sometimes differing by orders of magnitude, or to the beam qualities (energy spread and emittances) which are much worse in low-energy accelerators. For this reason some approximations, useful to treat high-energy undulator radiation, cannot be used in all cases. Just to give an example,

terms containing inverse powers of the electron energy should be retained in a correct treatment of the very low-energy undulator radiation. Furthermore the effects induced by the imperfect beam qualities, the so-called inhomogeneous broadening, cannot be ignored at all.

In this paper we reconsider the calculation of the linearly polarized undulator brightness, using analytical means and showing that one can go further than the usual approximation including corrections [3] up to the order $1/\gamma^3$ and studying the distortion induced in the radiated spectrum by the combined effects of the off-axis motion and of the magnet inhomogeneities.

An essential tool of the present analytical approach will be a class of generalized Bessel functions (GBF's) which will allow a synthetic and insightful approach to the problem [4].

II. UNDULATOR BRIGHTNESS, INCLUSION OF $(K/\gamma)^3$ CONTRIBUTIONS, AND GENERALIZED BESSEL FUNCTIONS

In the introductory part of this section we sketch the well-known derivation of the linear undulator spectrum, mainly to show how GBF's come into play and what is the simplification induced in the analysis.

We recall that the energy radiated per unit solid angle and frequency interval, in other words the brightness, is given by the well-known expression [5]

$$\frac{d^2 I}{d\Omega d\omega} = \frac{e^2 \omega^2}{4\pi^2 c} \left| \int_{-\infty}^{+\infty} \mathbf{n} \times (\mathbf{n} \times \boldsymbol{\beta}) \times \exp \left[i\omega \left(t - \frac{\mathbf{n} \cdot \mathbf{r}}{c} \right) \right] dt \right|^2, \quad (2.1)$$

where \mathbf{n} is a unit vector determining the direction of observation, \mathbf{r} refers to the particle position, and β to its reduced velocity. We assume that the electron moves in an undulator with N periods and with the magnetic-field distribution which, very near the axis, varies along z with the following sinusoidal dependence:

$$\mathbf{B} = B_0 \left[0, \sin \left[\frac{2\pi z}{\lambda_u} \right], 0 \right] \quad (2.2)$$

with λ_u being the undulator period.

The equations of motion for an electron moving in such a field can be easily obtained. Keeping contributions up to the second order in γ^{-1} (see Appendix A), one gets

$$\begin{aligned} \mathbf{r}(t) &= \left[\frac{c}{\tilde{\Omega}_u} \frac{K}{\gamma} \sin(\tilde{\Omega}_u t), 0, \beta^* ct \right. \\ &\quad \left. - \frac{1}{8} \left[\frac{K}{\gamma} \right]^2 \frac{c}{\tilde{\Omega}_u} \sin(2\tilde{\Omega}_u t) \right], \\ \beta^* &= 1 - \frac{1}{2\gamma^2} \left[1 + \frac{K^2}{2} \right], \quad K = \frac{eB_0 \lambda_u}{2\pi m_0 c^2}, \quad (2.3) \\ \Omega_u &= \frac{2\pi c}{\lambda_u}, \quad \tilde{\Omega}_u = \Omega_u \beta_z, \end{aligned}$$

where K is the so-called undulator parameter, usually of the order of unity. Since the emission angle is of the order of K/γ , we obtain

$$\mathbf{n} \equiv (\psi \cos \phi, \psi \sin \phi, 1 - \frac{1}{2}\psi^2) \quad (2.4)$$

and therefore

$$\begin{aligned} \mathbf{n} \cdot \mathbf{r} &\cong \frac{c}{\tilde{\Omega}_u} \frac{K}{\gamma} \psi \cos(\phi) \sin(\tilde{\Omega}_u t) \\ &\quad + (1 - \frac{1}{2}\psi^2) \beta^* ct - \frac{1}{8} \frac{c}{\tilde{\Omega}_u} \left[\frac{K}{\gamma} \right]^2 \sin(2\tilde{\Omega}_u t) \end{aligned} \quad (2.5)$$

and

$$\begin{aligned} [\mathbf{n} \times (\mathbf{n} \times \beta \times)]_x &\cong \psi \cos(\phi) - \frac{K}{\gamma} \cos(\tilde{\Omega}_u t), \\ [\mathbf{n} \times (\mathbf{n} \times \beta)]_y &\cong \psi \sin(\phi), \\ [\mathbf{n} \times (\mathbf{n} \times \beta)]_z &\cong \frac{K}{\gamma} \psi \cos(\phi) \cos(\tilde{\Omega}_u t) - \psi^2. \end{aligned} \quad (2.6)$$

In deriving both Eqs. (2.5) and (2.6) we have neglected terms $o((K/\gamma)^n)$ with $n \geq 3$. The oscillating part in Eq. (2.1) can be written in the form

$$\exp \left[i\omega \left(t - \frac{\mathbf{n} \cdot \mathbf{r}}{c} \right) \right] \cong \sum_{m=-\infty}^{+\infty} \exp \left\{ i \left[\frac{\omega}{2\gamma^2} \left(1 + \frac{K^2}{2} + \gamma^2 \psi^2 \right) - m \tilde{\Omega}_u \right] t \right\} J_m(Z_\omega, -\xi_\omega), \quad (2.7)$$

where we have defined

$$\begin{aligned} Z_\omega &= (K/\gamma)(\omega/\tilde{\Omega}_u) \psi \cos(\phi), \\ \xi_\omega &= \frac{1}{8}(K/\gamma)^2(\omega/\tilde{\Omega}_u). \end{aligned} \quad (2.8)$$

The function $J_m(x, y)$ is the GBF of the first kind whose properties are discussed in Appendix B and whose generating function is provided by [4]

$$\sum_{m=-\infty}^{+\infty} t^m J_m(x, y) = \exp \left[\frac{x}{2} \left(t - \frac{1}{t} \right) + \frac{y}{2} \left(t^2 - \frac{1}{t^2} \right) \right].$$

The integral over time in Eq. (2.1) can be factorized out and integrating from 0 to $L_u/c\beta_z = 2\pi N/\tilde{\Omega}_u$, where an effective acceleration exists, we get

$$\begin{aligned} H_m(v_m) &= \int_0^{2\pi N/\tilde{\Omega}_u} dt \exp \left\{ i \left[\frac{\omega}{2\gamma^2} \left(1 + \frac{K^2}{2} + \gamma^2 \psi^2 \right) \right. \right. \\ &\quad \left. \left. - m \tilde{\Omega}_u \right] t \right\} \\ &= \frac{2\pi N}{\tilde{\Omega}_u} \left[\frac{\sin(mv_m/2)}{mv_m/2} \right] \exp(-imv_m/2), \quad (2.9) \end{aligned}$$

where

$$\begin{aligned} \omega_m &= \frac{2\gamma^2 \tilde{\Omega}_u m}{1 + K^2/2 + \gamma^2 \psi^2} \cong \frac{2\gamma^2 \Omega_u m}{1 + K^2/2 + \gamma^2 \psi^2}, \\ v_m &= 2\pi N \left[\frac{\omega_m - \omega}{\omega_m} \right]. \end{aligned} \quad (2.10)$$

It is now easy to show that

$$\frac{d^2 I}{d\omega d\Omega} = \frac{e^2}{4\pi^2 c} \sum_m \omega_m^2 |H_m(v_m)|^2 (|T_m^x|^2 + |T_m^y|^2) \quad (2.11)$$

where

$$\begin{aligned} T_m^x &= \psi \cos(\phi) J_m(mZ, -m\xi) \\ &\quad - \frac{K}{2\gamma} [J_{m+1}(mZ, -m\xi) + J_{m-1}(mZ, -m\xi)], \\ T_m^y &= \psi \sin(\phi) J_m(mZ, -m\xi). \end{aligned} \quad (2.12)$$

The quantities $T_m^{x,y}$ are the radial and vertical components of the radiated spectrum. The expression usually given in the literature is easily recovered, noticing that (see Appendix B)

$$J_m(x, y) = \sum_{l=-\infty}^{+\infty} J_{m-2l}(x) J_l(y). \quad (2.13)$$

The advantages offered by the GBF's are both analytical and computational and become more evident when GBF's with larger numbers of variables are involved (see Sec. III and Appendix B for further details).

The expression (2.11) has been derived in the large- N limit, assuming that the spectrum consists essentially in a series of isolated peaks and by replacing, in Eqs. (2.11) and (2.12), ω by ω_m . In the large N -limit we have indeed

$$\left[\frac{\sin[\pi N(\omega/\omega_1 - m)]}{\pi N(\omega/\omega_1 - m)} \right]^2 \xrightarrow{N \rightarrow \infty} \delta \left[\frac{\omega}{\omega_1} - m \right]. \quad (2.14)$$

However, the assumption still holds for relatively low- N values when the harmonics are not overlapping.

With this substitution the expressions for Z and ξ in Eq. (2.8), turn into

$$\xi = \frac{K^2/4}{1 + K^2/2 + \gamma^2 \psi^2}, \quad (2.15)$$

$$Z = \frac{2K\gamma\psi \cos(\phi)}{1 + K^2/2 + \gamma^2 \psi^2}. \quad (2.16)$$

The frequency selection is immediately understood. In fact, from Eq. (2.11), it follows that the width of each harmonic contribution is inversely proportional to the number of undulator periods.

We have stressed that the above results are valid only when contributions of the order of $(K/\gamma)^n$, with $n \geq 3$, are neglected.

Sometimes, when the undulator radiation brightness produced by a low-energy electron beam is analyzed, such an assumption is not fully justified. It is therefore worth including higher-order corrections, which also provide a more accurate control of the above-quoted approximation. The analysis of the brightness including terms of the order of $(K/\gamma)^4$ is rather intriguing according to the above formalism. We therefore limit the present approach to the inclusion of $(K/\gamma)^3$ terms. Within this perturbative analysis the correction arises from the x component of motion, which now reads (see Appendix A)

$$x(t) \cong \frac{K}{\gamma} \frac{c}{\tilde{\Omega}_u} \sin(\tilde{\Omega}_u t) + \frac{1}{16} \left[\frac{K}{\gamma} \right]^3 \frac{c}{\tilde{\Omega}_u} [\sin(\tilde{\Omega}_u t) - \frac{1}{3} \sin(3\tilde{\Omega}_u t)], \quad (2.17)$$

$$\beta_x(t) = \frac{K}{\gamma} \cos(\tilde{\Omega}_u t) + \frac{1}{16} \left[\frac{K}{\gamma} \right]^3 [\cos(\tilde{\Omega}_u t) - \cos(3\tilde{\Omega}_u t)]. \quad (2.18)$$

As shown in Appendix A, the z component remains the same as that given in Eq. (2.3), since it contains even powers of (K/γ) only.

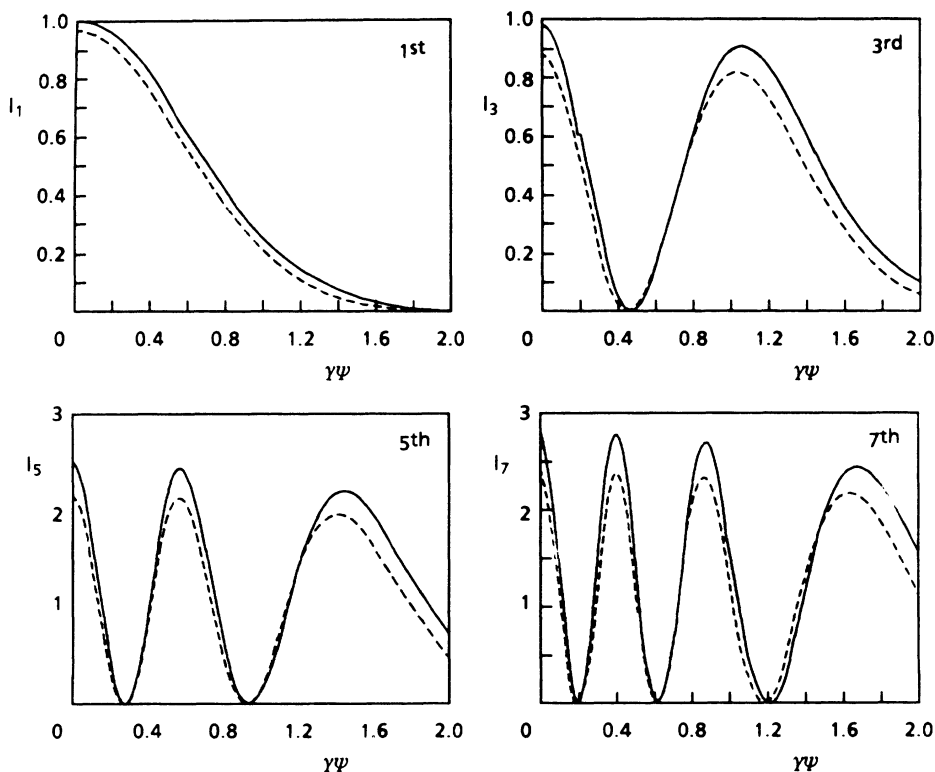


FIG. 1. Brightness vs $\gamma\psi$ for the first odd harmonic ($k=3$ and $\gamma=5$); continuous line; this theory; dotted line; ultrarelativistic approximation.

The derivation of the brightness is straightforward, the only problem is computational due to a larger number of terms to be retained. The vector \mathbf{n} now writes

$$\mathbf{n} \equiv \left(\left(\psi - \frac{1}{6} \psi^3 \right) \cos(\phi), \left(\psi - \frac{1}{6} \psi^3 \right) \sin(\phi), 1 - \frac{1}{2} \psi^2 \right). \quad (2.19)$$

Limiting the expansion up to the third order in K/γ the exponential term in (2.1) is still given by Eq. (2.7). On the other hand, the effect of this approximation appears in a more complicated structure of the following expression:

$$\begin{aligned} [\mathbf{n} \times (\mathbf{n} \times \boldsymbol{\beta})]_x \cong & \left[1 - \frac{1}{2\gamma^2} \left[1 + \frac{K^2}{2} + \frac{4}{3} \gamma^2 \psi^2 \right] \right] \psi \cos(\phi) - \frac{K}{\gamma} \left[1 - \psi^2 \cos^2(\phi) + \frac{1}{16} \left[\frac{K}{\gamma} \right]^2 \right] \cos(\tilde{\Omega}_u t) \\ & - \frac{1}{4} \left[\frac{K}{\gamma} \right]^2 \psi \cos(\phi) \cos(2\tilde{\Omega}_u t) + \frac{1}{16} \left[\frac{K}{\gamma} \right]^3 \cos(3\tilde{\Omega}_u t), \end{aligned} \quad (2.20)$$

$$[\mathbf{n} \times (\mathbf{n} \times \boldsymbol{\beta})]_y \cong \left[1 - \frac{1}{2\gamma^2} \left[1 + \frac{K^2}{2} + \frac{4}{3} \gamma^2 \psi^2 \right] \right] \psi \sin(\phi) + \frac{1}{2} \frac{K}{\gamma} \psi^2 \sin(2\phi) \cos(\tilde{\Omega}_u t) - \frac{1}{4} \left[\frac{K}{\gamma} \right]^2 \psi \sin(\phi) \cos(2\tilde{\Omega}_u t),$$

$$[\mathbf{n} \times (\mathbf{n} \times \boldsymbol{\beta})]_z \cong -\psi^2 + \frac{K}{\gamma} \psi \cos(\phi) \cos(\tilde{\Omega}_u t).$$

In analogy to what has been done previously, we define

$$\begin{aligned} T_m^x = & \left[1 - \frac{1}{2\gamma^2} \left[1 + \frac{K^2}{2} + \frac{4}{3} \gamma^2 \psi^2 \right] \right] \psi \cos(\phi) J_m(\mathbf{Z}, -\xi) \\ & - \frac{1}{2} \frac{K}{\gamma} \left[1 - \psi^2 \cos^2(\phi) - \frac{1}{16} \left[\frac{K}{\gamma} \right]^2 \right] [J_{m+1}(\mathbf{Z}, -\xi) + J_{m-1}(\mathbf{Z}, -\xi)] \\ & - \frac{1}{8} \left[\frac{K}{\gamma} \right]^2 \psi \cos(\phi) [J_{m+2}(\mathbf{Z}, -\xi) + J_{m-2}(\mathbf{Z}, -\xi)] + \frac{1}{32} \left[\frac{K}{\gamma} \right]^3 [J_{m+3}(\mathbf{Z}, -\xi) + J_{m-3}(\mathbf{Z}, -\xi)], \\ T_m^y = & \psi \sin(\phi) \left[1 - \frac{1}{2\gamma^2} \left[1 + \frac{K^2}{2} + \frac{4}{3} \gamma^2 \psi^2 \right] \right] J_m(\mathbf{Z}, -\xi) + \frac{1}{4} \frac{K}{\gamma} \psi^2 \sin(2\phi) [J_{m+1}(\mathbf{Z}, -\xi) + J_{m-1}(\mathbf{Z}, -\xi)] \\ & - \frac{1}{8} \left[\frac{K}{\gamma} \right]^2 \psi \sin(\phi) [J_{m+2}(\mathbf{Z}, -\xi) + J_{m-2}(\mathbf{Z}, -\xi)], \end{aligned} \quad (2.21)$$

$$T_m^z = -\psi^2 J_m(\mathbf{Z}, -\xi) + \frac{1}{2} \frac{K}{\gamma} \psi \cos(\phi) [J_{m+1}(\mathbf{Z}, -\xi) + J_{m-1}(\mathbf{Z}, -\xi)].$$

The integral on time can be worked out straightforwardly, thus finding

$$\frac{d^2 I}{d\omega d\Omega} = \frac{e^2}{4\pi^2 c} \sum_m \omega_m^2 |H_m(v_m)|^2 (|T_m^x|^2 + |T_m^y|^2 + |T_m^z|^2), \quad (2.22)$$

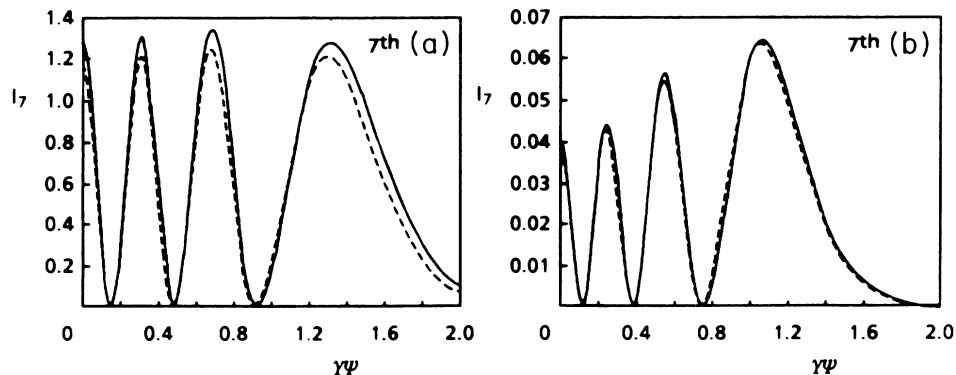


FIG. 2. Seventh harmonic brightness, (a) $k=2$, $\gamma=5$; (b) $k=1$, $\gamma=5$.

where $H_m(v_m)$ is specified in (2.9).

To appreciate the difference with respect to the previously discussed case we consider the on-axis emission ($\psi=0$). The only surviving term in Eqs. (2.21) is the radial polarization, which reads

$$T_m^x = \frac{(-1)^{(m-1)/2}}{2} \frac{K}{\gamma} \left\{ \left[1 + \frac{1}{16} \left(\frac{K}{\gamma} \right)^2 \right] [J_{(m-1)/2}(\xi) - J_{(m+1)/2}(\xi)] + \frac{1}{16} \left(\frac{K}{\gamma} \right)^2 [J_{(m-3)/2}(\xi) - J_{(m+3)/2}(\xi)] \right\} \quad (2.23)$$

and m takes odd values only. We find therefore that on-axis odd harmonics only are emitted and in addition to the nearest-neighbor index contributions $[(m \pm 1)/2]$ we have also those deriving from indices $[(m \pm 3)/2]$. The physical reasons underlying the appearance of those terms are due to the $3\bar{\Omega}_u$ modulation in x motion. The possibility of observing new contributions is however limited to low-energy and high- K cases.

The effect of the low-energy corrections on the undulator brightness is better clarified by Figs. 1, 2, and 3, we compare the results of the present analysis with those not including the $(K/\gamma)^3$ corrections. As already stressed the importance of the corrections is more evident at lower energies, higher K , and higher harmonics. In the case of $K=3$ and $\gamma=5$, the correction is larger than 10%.

III. UNDULATOR BRIGHTNESS AND OFF-AXIS MOTION

The undulator field is correctly reproduced by Eq. (2.2) only near the undulator axis, otherwise the dependence on the transverse coordinates should be included, to satisfy the Maxwell's equations [6]. The modification induced in the field and the appearance of nonzero contributions from multipolar elements, both in vertical and radial

directions, produces distortion in the electron trajectory, which consists of the reference term (2.3) and of a slow motion due to the multipolar contributions (see Appendix A).

In general we have

$$x = x_R + x_1, \quad y = y_R + y_1. \quad (3.1)$$

Since, in the present case, $y_R=0$, the vertical motion will be provided by the "slow" component y_1 only. When the electron motion is focused in both directions, the extra motion (x_1, y_1) is given by

$$\begin{aligned} x_1 &= x_1(0) \cos(\Omega_1 t) + \frac{\dot{x}_1(0)}{\Omega_1} \sin(\Omega_1 t), \\ y_1 &= y_1(0) \cos(\Omega_2 t) + \frac{\dot{y}_1(0)}{\Omega_2} \sin(\Omega_2 t), \end{aligned} \quad (3.2)$$

where

$$\Omega_{1,2} = \frac{K}{2\gamma} \Omega_u \sqrt{h_{1,2}}, \quad h_{1,2} = \delta, \quad 2 - \delta \quad (3.3)$$

and δ is the sextupolar term, assumed positive to ensure focusing in both directions. The longitudinal component, calculated from the total velocity conservation, writes

$$\begin{aligned} z &= \beta^{**} ct + \frac{1}{4c} [x_1(0)\dot{x}_1(0) + y_1(0)\dot{y}_1(0)] - \frac{K}{\gamma} \frac{\Omega_1^2}{\Omega_u^2 - \Omega_1^2} x_1(0) - \frac{c}{8\Omega_u} \left(\frac{K}{\gamma} \right)^2 \sin(2\Omega_u t) \\ &\quad - \frac{1}{2} \mathcal{L}_x \sin(2\Omega_1 t) - \frac{1}{4c} x_1(0)\dot{x}_1(0) \cos(2\Omega_1 t) - \frac{1}{2} \mathcal{L}_y \sin(2\Omega_2 t) - \frac{1}{4c} y_1(0)\dot{y}_1(0) \cos(2\Omega_2 t) \\ &\quad - \frac{K}{2\gamma} \left\{ \frac{1}{\Omega_u - \Omega_1} \{ \dot{x}_1(0) \sin[(\Omega_u - \Omega_1)t] - \Omega_1 x_1(0) \cos[(\Omega_u - \Omega_1)t] \} \right. \\ &\quad \left. + \frac{1}{\Omega_u + \Omega_1} \{ \dot{x}_1(0) \sin[(\Omega_u + \Omega_1)t] + \Omega_1 x_1(0) \cos[(\Omega_u + \Omega_1)t] \} \right\} \end{aligned} \quad (3.4)$$

where

$$\begin{aligned} \mathcal{L}_\eta(\cdot) &= \frac{1}{4c\Omega_\eta} \{ \dot{\eta}^2(0) - [\eta(0)\Omega_\eta]^2 \}, \quad \eta = x, y, \\ \beta^{**} &= \beta^* - \frac{1}{2c^2} [H_x(0) + H_y(0)], \quad H_\eta = \frac{1}{2} [\dot{\eta}^2 + (\Omega_\eta \eta)^2]. \end{aligned} \quad (3.5)$$

The quantity H_η is a constant of motion.

A few words to explain the physical meaning of the above results are necessary. The initial conditions $(\eta(0), \dot{\eta}(0))$ are the off-axis initial position and velocity, the existence of a transverse gradient in the off-axis field induces the extramotion, which also modifies the average velocity β^* . We can therefore expect a change in the res-

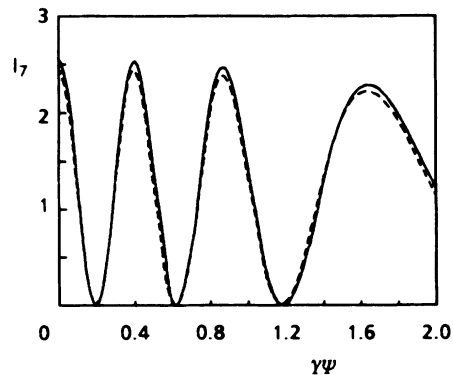


FIG. 3. Seventh harmonic brightness $k=2$, $\gamma=10$.

onance condition, through the Hamiltonians $H_{x,y}$ (see Appendix A). This last effect provides the basis for the so-called inhomogeneous broadening. We will limit the present analysis to the inclusion of $(K/\gamma)^2$ contributions, thus obtaining for the exponential term the Lienard-Wiechert integral (2.1)

$$\begin{aligned} \exp \left[i\omega \left(t - \frac{\mathbf{n} \cdot \mathbf{r}}{c} \right) \right] &= \exp \left[\frac{i\omega}{4c^2} [x_1(0)\dot{x}_1(0) + y_1(0)\dot{y}_1(0)] - \frac{i\omega K}{c} \frac{\Omega_1^2}{\Omega_u^2 - \Omega_1^2} x_1(0) \right] \\ &\times \sum_{m,n,p,k,l} \exp \left[i \left\{ \omega \left[1 - \beta^{**} \left(1 - \frac{\psi^2}{2} \right) \right] - [m\Omega_u + n\Omega_1 + p\Omega_2 + k(\Omega_u - \Omega_1) + l(\Omega_u + \Omega_1)] \right\} t \right] \\ &\times J_m \left[\frac{\omega K}{\Omega_u} \frac{\psi \cos(\phi)}{\gamma}, -\frac{1}{8} \left[\frac{K}{\gamma} \right]^2 \frac{\omega}{\Omega_u} \right] \\ &\times \mathcal{D}_n \left[-i\frac{\omega}{c} x_1(0)\psi \cos(\phi), i\frac{\omega}{4c^2} x_1(0)\dot{x}_1(0), \frac{\omega}{\Omega_1} \frac{\dot{x}_1(0)}{c} \psi \cos(\phi), -\frac{\omega}{2c} \mathcal{L}_x(0) \right] \\ &\times \mathcal{D}_p \left[-i\frac{\omega}{c} y_1(0)\psi \sin(\phi), i\frac{\omega}{4c^2} y_1(0)\dot{y}_1(0), \frac{\omega}{\Omega_2} \frac{\dot{y}_1(0)}{c} \psi \sin(\phi), -\frac{\omega}{2c} \mathcal{L}_y(0) \right] \\ &\times \mathcal{D}_k \left[-i\frac{\omega K}{c} \frac{\Omega_1 x_1(0)}{2\gamma \Omega_u - \Omega_1}, 0, -\frac{\omega K}{c} \frac{\dot{x}_1(0)}{2\gamma \Omega_u - \Omega_1}, 0 \right] \\ &\times \mathcal{D}_l \left[i\frac{\omega K}{c} \frac{\Omega_1 x_1(0)}{2\gamma \Omega_u + \Omega_1}, 0, -\frac{\omega K}{c} \frac{\dot{x}_1(0)}{2\gamma \Omega_u + \Omega_1}, 0 \right]. \end{aligned} \tag{3.6}$$

With a self-explaining simplified notation we have

$$\exp \left[i\omega \left(t - \frac{\mathbf{n} \cdot \mathbf{r}}{c} \right) \right] = \sum_{m,n,p,k,l} \exp \left[i \left[v_{m,n,p,k,l} \frac{ct}{L} + \theta \right] \right] J_m(\dots) \mathcal{D}_n(X) \mathcal{D}_p(Y) \mathcal{D}_k(d) \mathcal{D}_l(s), \tag{3.7}$$

where

$$v_{m,n,p,k,l} = 2\pi N \frac{[\omega - m\omega_u - n\omega_1 - p\omega_2 - k(\omega_u - \omega_1) - l(\omega_u + \omega_1)]}{\omega_u}, \tag{3.8}$$

$$\omega_i = \frac{2\gamma^2 \Omega_i}{1 + K^2/2 + \gamma^2 \psi^2 + (\gamma^2/c^2)(H_x + H_y)}, \quad i = u, 1, 2$$

and

$$\mathcal{D}_n(x, y, z, u) = \sum_{l=-\infty}^{+\infty} I_{n-l}(x, y) J_l(z, u), \tag{3.9}$$

where $I_n(x, y)$ is a modified GBF of the first kind (see Appendix B).

Using the same notations as before we finally find

$$\begin{aligned}
T_{m,n,p,k,l}^x &= \left[\psi \cos(\phi) J_m(\dots) \mathcal{D}_n(X) - \frac{K}{2\gamma} [J_{m+1}(\dots) + J_{m-1}(\dots)] \mathcal{D}_n(X) \right. \\
&\quad \left. - \frac{1}{2c} J_m(\dots) \{ \dot{x}_1(0) [\mathcal{D}_{n+1}(X) + \mathcal{D}_{n-1}(X)] + i\Omega_1 x_1(0) [\mathcal{D}_{n+1}(X) - \mathcal{D}_{n-1}(X)] \} \right] \mathcal{D}_p(Y) \mathcal{D}_k(d) \mathcal{D}_l(s), \\
T_{m,n,p,k,l}^y &= \left[\psi \sin(\phi) \mathcal{D}_p(Y) - \frac{1}{2c} \{ \dot{y}_1(0) [\mathcal{D}_{p+1}(Y) + \mathcal{D}_{p-1}(Y)] + i\Omega_2 y_1(0) [\mathcal{D}_{p+1}(Y) - \mathcal{D}_{p-1}(Y)] \} \right] \\
&\quad \times J_m(\dots) \mathcal{D}_n(X) \mathcal{D}_k(d) \mathcal{D}_l(s), \\
T_{m,n,p,k,l}^z &= \left[\psi \cos(\phi) \frac{K}{2\gamma} [J_{m+1}(\dots) + J_{m-1}(\dots)] \mathcal{D}_n(X) \mathcal{D}_p(Y) \right. \\
&\quad + \frac{\psi \cos(\phi)}{2c} \{ \dot{x}_1(0) [\mathcal{D}_{n+1}(X) + \mathcal{D}_{n-1}(X)] + i\Omega_1 x_1(0) [\mathcal{D}_{n+1}(X) - \mathcal{D}_{n-1}(X)] \} J_m(\dots) \mathcal{D}_p(Y) \\
&\quad + \frac{\psi \sin(\phi)}{2c} \{ \dot{y}_1(0) [\mathcal{D}_{p+1}(Y) + \mathcal{D}_{p-1}(Y)] + i\Omega_2 y_1(0) [\mathcal{D}_{p+1}(Y) - \mathcal{D}_{p-1}(Y)] \} J_m(\dots) \mathcal{D}_n(X) \\
&\quad \left. - \psi^2 J_m(\dots) \mathcal{D}_n(X) \mathcal{D}_p(Y) \right] \mathcal{D}_k(d) \mathcal{D}_l(s). \tag{3.10}
\end{aligned}$$

Introducing the function

$$\mathcal{H}_{m,n,p,k,l} = \frac{2\pi N}{\Omega_u} \frac{\sin(v_{m,n,p,k,l}/2)}{v_{m,n,p,k,l}/2} \exp(iv_{m,n,p,k,l}/2), \tag{3.11}$$

we can write the brightness as

$$\frac{d^2 I}{d\omega d\Omega} = \frac{e^2}{4\pi^2 c} \sum_{\{i\}} \omega^2 (|T_{\{i\}}^x|^2 + |T_{\{i\}}^y|^2 + |T_{\{i\}}^z|^2) \mathcal{H}_{\{i\}}^2, \quad \{i\} = m, n, p, k, l. \tag{3.12}$$

The results we have obtained show the existence of a much richer phenomenology whose physical aspects are not difficult to understand.

The inclusion of the betatron contributions gives a very clear idea of how the off-axis motion induces not only a shift of the central emission frequency but also a variation in the intensity radiated at a fixed harmonic. The outlined procedure provides the basis for a more complete understanding of the inhomogeneous broadening effects, once the whole structure of the electron beam is accounted for. One of the most significant results of the above analysis has been an analytically quantitative determination of how the off-axis injection allows even harmonics to be emitted on axis.

Let us consider, for instance, the case

$$x_1(0) = x_0, \quad \dot{x}_1(0) = y_1(0) = \dot{y}_1(0) = 0. \tag{3.13}$$

From the properties of the GBF (see Appendix B) it follows that $|T_{m,n,p,k,l}^x|^2$, for m even, writes as

$$\begin{aligned}
|T_{m,n,p,k,l}^x|^2 &= J_k^2(\gamma_-) J_l^2(\gamma_+) \left[\left[\frac{K}{2\gamma} \right]^2 [J_{(m-1)/2}(\xi) - J_{(m+1)/2}(\xi)]^2 J_{n/2}^2(\xi_\beta) \right. \\
&\quad \left. + \left[\frac{\Omega_1 x_0}{2c} \right]^2 [J_{(n-1)/2}(\xi_\beta) - J_{(n+1)/2}(\xi_\beta)]^2 J_{m/2}^2(\xi) \right], \tag{3.14a}
\end{aligned}$$

where

$$\begin{aligned}\xi &= \frac{1}{8} \frac{\omega}{\Omega_u} \left(\frac{K}{\gamma} \right)^2, \\ \xi_\beta &= \frac{1}{8} \frac{\omega}{\Omega_u} \left(\frac{2H_1}{c^2} \right) = \frac{1}{8} \frac{\omega \Omega_1 x_0^2}{c^2}, \\ \gamma_\pm &= \frac{K}{2\gamma} \frac{\Omega_1 x_0}{c} \frac{\omega}{\Omega_u \pm \Omega_1}.\end{aligned}\quad (3.14b)$$

The result of such an extra modulation is that the carrier harmonic m has a further substructure provided by the harmonics indexed with n .

The above analysis is relevant to, a single electron and makes sense if the electron executes many betatron oscillations while traversing the undulator. If we consider just the natural undulator focusing with $h_1 = h_2 = 1$, the following condition should be satisfied:

$$\lambda_\beta = \frac{\gamma \lambda_u}{K} \ll N \lambda_u, \quad (3.15)$$

which is easily verified in the low-energy case. Furthermore if one includes one contribution of all the electrons in the beam, inhomogeneous broadening effects may arise, which broaden the linewidth and reduce the peaks of the radiated betatron harmonics. To appreciate the importance of this contribution we notice that the relative ‘‘inhomogeneous’’ bandwidth of the first betatron harmonic $\lambda_{0,1,0,0,0}$ is

$$\left(\frac{\Delta\omega}{\omega} \right)_\beta = \left(\frac{1}{2N} \right) \frac{\gamma}{K}, \quad (3.16)$$

which is significantly larger than the homogeneous linewidth for, e.g., the harmonics $\lambda_{1,0,0,0,0}$. Within this respect the effect of inhomogeneous broadening caused, e.g., by the beam energy spread and emittances should be less severe than that affecting the undulator harmonics.

This paper is by no means complete. We did not discuss, in fact, the problems relevant to, e.g., defocusing cases or those associated with helical undulators. The defocusing (in one direction) undulator case can be easily included in the present analysis; it is just a matter of being careful with the GBF's appearing in the spectrum. The helical undulator problem is by far more complicated owing to the existence in the (x_1, y_1) motion equations of solenoidal coupling terms.

$$\omega_{m,n,p,k,l} = \frac{2\gamma^2 [m\Omega_u + n\Omega_1 + p\Omega_2 + k(\Omega_u - \Omega_1) + l(\Omega_u - \Omega_2)]}{1 + K^2/2 + (\gamma\psi)^2 + (\gamma/c)^2(H_x + H_y)}. \quad (4.2)$$

We have therefore, in principle, an extraordinarily intrigued spectroscopic structure of the undulator spectrum whose physical origin must be traced back to the various harmonic contents of the electron motion and to their

IV. CONCLUDING REMARKS

In this paper we have shown that analytical progress can be done in the analysis of undulator radiation including in the computation low-energy effects and the betatron motion components. A crucial step in our work consists of the use of the GBF's which are the natural mathematical tool for this kind of analysis.

The results we have obtained do not show, however, any dramatic impact on what is already known and the magnitudes of the low-energy corrections show that the usual approximations can be safely used even for electron energy around 5 MeV and $K \cong 2$. We did not find deviations, at least up to $(K/\gamma)^3$, from the usual resonance conditions. However, in a forthcoming paper, it will be shown that, including $(K/\gamma)^4$ terms, the central emission wavelength reads

$$\lambda_1 \cong \frac{\lambda_u}{2\gamma^2} \left[1 + \frac{K^2}{2} + \frac{3}{4\gamma^2} (1 + K^2 + \frac{3}{8}K^4) \right], \quad (4.1)$$

which, for electron energies around 2–3 MeV, can give significant deviations (some percent, depending on K) from those predicted with the usual formula.

We have also seen that, with the inclusion of $(K/\gamma)^3$ terms, the on-axis emission pattern is slightly more complicated since an entirely new contribution appears containing Bessel functions of the order $J_{(m+3)/2}$ (m odd). We have already noticed that the physical reasons underlying such new terms are due to the fact that the transverse electron motion has an oscillatory component at the frequency $3\tilde{\Omega}_u$. This oscillatory term is a further contribution beyond the usual dipole approximation, and the electron trajectory, in a frame moving at the speed $\beta_z \cong 1 + 1/2\gamma^2(1 + K^2)$, has not the well-known eight-like structure, but further lobes appear.

We have numerically checked some of the above results using the S-LUCE code [2], finding agreement with the above predictions. In particular, at low energies, we found a systematic shift of the central peak of each harmonic resonance, consistent with Eq. (4.1).

Betatron harmonics have been the second topic of the paper. The effects due to the off-axis structure of the undulator have been included in the calculation of brightness and, although the mathematics is quite complicated, it has been possible to get general expressions and perhaps a deeper understanding of the role played by the inhomogeneous broadening effects. We have noticed that inclusion of the betatron motion induces a richer harmonic content in the spectrum.

One of the main conclusions of the present analysis is that many harmonics can operate and that the resonance condition is provided by

mutual interference.

Let us, however, better explore the physical contents of Eq. (4.2) and consider first the case

$$\omega_{m,0,0,0,0} = \frac{2m\gamma^2\Omega_u}{1+K^2/2+\gamma^2[\psi^2+(H_x+H_y)/c^2]} \quad (4.3)$$

The new term appearing at the denominator $(1/c^2)(H_x+H_y)$ is a kind of correction to the emission angle ψ and is just due to the off-axis injection angle [or velocity (\dot{x}, \dot{y})] and to the transverse spring force [see Eq. (3.5)].

The above term gives a shift from the usual resonance condition, which is the source of the usual inhomogeneous broadening effects treated, within a different framework, in Ref. [6]. The usual analytical treatment of such effects is limited since it is essentially based on a convolution of the $(\sin^2 X)/X^2$ part of the spectrum without keeping into account the Bessel function content. The analysis we have presented allows the possibility of making a more general analytical treatment.

Equation (4.2) also predicts emission at lower frequencies than that usually referred to as the fundamental frequency, namely, $\omega_{1,0,0,0,0}$. We have, e.g.,

$$\omega_{0,0,1,0,0} = \frac{2\gamma^2\Omega_2}{1+K^2/2+(\gamma\psi)^2+(\gamma/c)^2(H_x+H_y)} \quad (4.3')$$

whose associated wavelength is

$$\lambda_{0,0,1,0,0} = \frac{\lambda_u}{\gamma} \frac{1+K^2/2+\gamma^2[\psi+(H_x+H_y)/c^2]}{K\sqrt{2-\delta}}, \quad (4.4)$$

which is 2γ times larger than the usual fundamental wavelength.

ACKNOWLEDGMENTS

It is a pleasure to recognize the important contribution given by Dr. C. Chiccoli, Dr. S. Lorenzutta, and Dr. G. Maino to the theory of the generalized Bessel functions widely exploited in this paper. Furthermore the authors express their gratitude to Dr. G. Voykov for a careful reading of the manuscript and for his deep and constructive criticism.

APPENDIX A: THE EQUATION OF MOTION FOR ELECTRONS MOVING IN A LINEARLY POLARIZED UNDULATOR MAGNET

1. Electron motion up to the third order in K/γ

We consider electrons moving in an undulator field with components given by Eq. (2.2) and assume that they are injected on axis with zero transverse position. From the Lorentz equation of motion we get

$$\ddot{z} = \frac{e\dot{x}}{m_0\gamma c} B_0 \sin \left[\frac{2\pi z}{\lambda_u} \right], \quad (A1)$$

$$\ddot{x} = -\frac{e\dot{z}}{m_0\gamma c} B_0 \sin \left[\frac{2\pi z}{\lambda_u} \right].$$

Since the velocity is a constant of motion we can immediately integrate the second of the above equations, thus obtaining

$$\beta_x = \frac{K}{\gamma} \cos \left[\frac{2\pi z}{\lambda_u} \right]. \quad (A2)$$

Furthermore we also have

$$\beta_z^2 = 1 - \frac{1}{\gamma^2} \left[1 + K^2 \cos^2 \left[\frac{2\pi z}{\lambda_u} \right] \right]. \quad (A3)$$

Expanding the square root of (A3) up to the third order we find

$$\beta_z \cong 1 - \frac{1}{2\gamma^2} \left[1 + K^2 \cos^2 \left[\frac{2\pi z}{\lambda_u} \right] \right]. \quad (A4)$$

The above expression can be written as

$$\beta_z = \langle \beta_z \rangle + \Delta\beta_z, \quad (A5)$$

where

$$\langle \beta_z \rangle = 1 - \frac{1}{2\gamma^2} \left[1 + \frac{K^2}{2} \right], \quad (A6a)$$

$$\Delta\beta_z = -\frac{K^2}{4\gamma^2} \cos \left[\frac{4\pi z}{\lambda_u} \right],$$

the longitudinal coordinate can be evaluated integrating the above expression, thus obtaining

$$\begin{aligned} z(t) &= \langle \beta_z \rangle ct - \frac{K^2 c}{4\gamma^2} \int_0^t \cos \left[\frac{4\pi z(t')}{\lambda_u} \right] dt' \\ &= z_0(t) + \Delta z(t). \end{aligned} \quad (A6b)$$

The oscillating term $\Delta z(t)$ can be expanded in series of K/γ since the function appearing in the integral is limited for all z . Considering terms up to the third order we have

$$\begin{aligned} \beta_z(t) &= \langle \beta_z \rangle - \frac{K^2}{4\gamma^2} \cos(2\tilde{\Omega}_u t), \\ z(t) &= \langle \beta_z \rangle ct - \frac{cK^2}{8\gamma^2} \sin(2\tilde{\Omega}_u t). \end{aligned} \quad (A7)$$

We can now calculate the relevant expression for β_x and x just using Eqs. (A6a) and (A6b) inserted into Eq. (A2), thus obtaining

$$\begin{aligned}\beta_x(t) &= \frac{K}{\gamma} \cos(\tilde{\Omega}_u t) + \frac{K^3}{16\gamma^3} [\cos(\tilde{\Omega}_u t) - \cos(3\tilde{\Omega}_u t)], \\ x(t) &= \frac{K}{\gamma} \frac{c}{\tilde{\Omega}_u} \sin(\tilde{\Omega}_u t) \\ &\quad + \frac{K^3}{16\gamma^3} \frac{c}{\tilde{\Omega}_u} [\sin(\tilde{\Omega}_u t) - \frac{1}{3}\sin(3\tilde{\Omega}_u t)].\end{aligned}\quad (\text{A8})$$

2. Betatron motion

We have already stressed that the field components (2.1) are accurate only near the undulator axis, otherwise, they do not satisfy Maxwell's equations. At lowest order in the transverse coordinates, the field components read [6]

$$\begin{aligned}B_x(x, y, z) &\cong 2B_0\delta \left[\frac{\pi}{\lambda_u} \right]^2 xy \sin \left[\frac{2\pi z}{\lambda_u} \right], \\ B_y(x, y, z) &\cong B_0 \left[1 + \left[\frac{\pi}{\lambda_u} \right]^2 [x^2\delta + y^2(2-\delta)] \right] \\ &\quad \times \sin \left[\frac{2\pi z}{\lambda_u} \right], \\ B_z(x, y, z) &\cong B_0 \frac{2\pi}{\lambda_u} y \cos \left[\frac{2\pi z}{\lambda_u} \right].\end{aligned}\quad (\text{A9})$$

The equations of motion can be now derived using the field distribution (A9), which for the transverse motion yields

$$\begin{aligned}\ddot{x} &= -\frac{eB_0}{m_0\gamma c} \dot{z} \sin \left[\frac{2\pi z}{\lambda_u} \right] \\ &\quad - \frac{eB_0}{m_0\gamma c} \left[\frac{\pi}{\lambda_u} \right]^2 [\delta x^2 + (2-\delta)y^2] \dot{z} \sin \left[\frac{2\pi z}{\lambda_u} \right] \\ &\quad + \frac{2\pi}{\lambda_u} y \dot{y} \frac{eB_0}{m_0\gamma c} \cos \left[\frac{2\pi z}{\lambda_u} \right], \\ \ddot{y} &= -\frac{eB_0}{m_0\gamma c} \left[\frac{2\pi}{\lambda_u} \dot{x} y \cos \left[\frac{2\pi z}{\lambda_u} \right] \right. \\ &\quad \left. - \left[\frac{\pi}{\lambda_u} \right]^2 2\delta xy \dot{z} \sin \left[\frac{2\pi z}{\lambda_u} \right] \right].\end{aligned}\quad (\text{A10})$$

According to what we have discussed in Sec. III, we assume that the motion can be decomposed as follows:

$$x = x_R + x_1, \quad y = y_R + y_1, \quad (\text{A11})$$

where (x_R, y_R) specify the "reference" trajectory due to the field (2.2) and (x_1, y_1) describe the additional motion around the reference trajectory due to the extra terms in (A9) depending on the transverse coordinates. Assuming the motion around the reference trajectory small once compared with (x_R, y_R) , keeping contributions only at the first order in (x_1, y_1) in Eq. (A12) and averaging on the undulator period, we get the following differential equations specifying the additional motion (the prime denotes derivation with respect to $s = ct$):

$$\begin{aligned}x_1'' &= - \left[\frac{\pi K}{\lambda_u \gamma} \right]^2 \delta x_1, \\ y_1'' &= - \left[\frac{\pi K}{\lambda_u \gamma} \right]^2 (2-\delta) y_1.\end{aligned}\quad (\text{A12})$$

The above equations state that the undulator acts as an optical element focusing in both radial and vertical directions when $\delta > 0$, otherwise it is vertically focusing and radially defocusing.

The solutions of Eq. (A12) are straightforward and read

$$\begin{aligned}x_1 &= x_1(0) \cos(\Omega_1 t) + \frac{\dot{x}_1(0)}{\Omega_1} \sin(\Omega_1 t), \\ y_1 &= y_1(0) \cos(\Omega_2 t) + \frac{\dot{y}_1(0)}{\Omega_2} \sin(\Omega_2 t),\end{aligned}\quad (\text{A13})$$

where

$$\Omega_1 = \frac{1}{2}\sqrt{\delta} \frac{K}{\gamma} \Omega_u, \quad \Omega_2 = \frac{1}{2}\sqrt{2-\delta} \frac{K}{\gamma} \Omega_u, \quad (\text{A14})$$

and $(x_1(0), y_1(0); \dot{x}_1(0), \dot{y}_1(0))$ are the initial off-axis transverse positions and velocities.

The variations, induced by the off-axis motion on the longitudinal velocity, are obtained from the condition

$$\dot{x}^2 + \dot{y}^2 + \dot{z}^2 = \beta^2 c^2, \quad (\text{A15})$$

therefore deriving

$$\begin{aligned}\dot{z} &= \beta c \left[1 - \frac{1}{2} \left[\frac{K^2}{\beta^2 c^2} \cos^2(\Omega_u t) + \frac{1}{\beta^2 c^2} [-x_1(0)\Omega_1 \sin(\Omega_1 t) + \dot{x}_1(0)\cos(\Omega_1 t)]^2 \right. \right. \\ &\quad \left. \left. + 2 \frac{K}{\beta^2 \gamma c} \cos(\Omega_u t) [-x_1(0)\Omega_1 \sin(\Omega_1 t) + \dot{x}_1(0)\cos(\Omega_1 t)] \right. \right. \\ &\quad \left. \left. + \frac{1}{\beta^2 c^2} [-y_1(0)\Omega_2 \sin(\Omega_2 t) + \dot{y}_1(0)\cos(\Omega_2 t)]^2 \right] \right]\end{aligned}\quad (\text{A16})$$

and

$$\begin{aligned}
z = \beta c t - \frac{1}{2} \beta c \left\{ \frac{K^2}{\gamma^2} \frac{1}{2\Omega_u} [\Omega_u t + \frac{1}{2} \sin(2\Omega_u t)] + \frac{1}{2c^2} \left[x_1^2(0) \Omega_1^2 \left[t - \frac{1}{2\Omega_1} \sin(2\Omega_1 t) \right] \right. \right. \\
\left. \left. + \dot{x}_1^2(0) \left[t + \frac{1}{2\Omega_1} \sin(2\Omega_1 t) \right] + 2x_1(0) \dot{x}_1(0) \sin^2(\Omega_1 t) \right] \right. \\
\left. + \frac{1}{2c^2} \left[y_1^2(0) \Omega_2^2 \left[t - \frac{1}{2\Omega_2} \sin(2\Omega_2 t) \right] + \dot{y}_1^2(0) \left[t + \frac{1}{2\Omega_2} \sin(2\Omega_2 t) \right] + 2y_1(0) \dot{y}_1(0) \sin^2(\Omega_2 t) \right] \right. \\
\left. + \frac{2K}{\gamma c} \left[-x_1(0) \Omega_1 \left[\frac{1 - \cos(\Omega_u - \Omega_1)t}{2(\Omega_u - \Omega_1)} - \frac{1 - \cos(\Omega_u + \Omega_1)t}{2(\Omega_u + \Omega_1)} \right] \right. \right. \\
\left. \left. + \dot{x}_1(0) \left[\frac{\sin(\Omega_u - \Omega_1)t}{2(\Omega_u - \Omega_1)} + \frac{\sin(\Omega_u + \Omega_1)t}{2(\Omega_u + \Omega_1)} \right] \right] \right\}. \quad (\text{A17})
\end{aligned}$$

APPENDIX B: GENERALIZED BESSEL FUNCTIONS

The generalized Bessel function [4] of the first kind is defined by the series expansion

$$J_n(x, y) = \sum_{l=-\infty}^{+\infty} J_{n-2l}(x) J_l(y) \quad (\text{B1})$$

and, as it is easily shown, it satisfies the following recurrence relations:

$$\begin{aligned}
\frac{\partial}{\partial x} J_n(x, y) &= \frac{1}{2} [J_{n-1}(x, y) - J_{n+1}(x, y)], \\
\frac{\partial}{\partial y} J_n(x, y) &= \frac{1}{2} [J_{n-2}(x, y) - J_{n+2}(x, y)], \quad (\text{B2}) \\
2nJ_n(x, y) &= x [J_{n-1}(x, y) + J_{n+1}(x, y)] \\
&\quad + 2y [J_{n-2}(x, y) + J_{n+2}(x, y)].
\end{aligned}$$

The generating function of $J_n(x, y)$, easily obtained, reads

$$\sum_{n=-\infty}^{+\infty} t^n J_n(x, y) = \exp \left[\frac{x}{2} \left[t - \frac{1}{t} \right] + \frac{y}{2} \left[t^2 - \frac{1}{t^2} \right] \right], \quad (\text{B3})$$

and the relevant Jacobi-Anger expansion writes as

$$\sum_{n=-\infty}^{+\infty} e^{in\theta} J_n(x, y) = \exp[i(x \sin\theta + y \sin 2\theta)]. \quad (\text{B4})$$

It is also easy to understand that

$$\begin{aligned}
J_n(x, 0) &= J_n(x), \quad J_n(0, 0) = \delta_{n,0}, \\
J_n(0, y) &= \begin{cases} J_{n/2}(y) & \text{for } n \text{ even} \\ 0 & \text{for } n \text{ odd.} \end{cases} \quad (\text{B5})
\end{aligned}$$

Furthermore, setting $t=1$ or $\theta=0$ in Eqs. (B3) and (B4) one has the following closure relation:

$$\sum_{n=-\infty}^{+\infty} J_n(x, y) = 1. \quad (\text{B6})$$

The following relations are of particular importance for computational purposes:

$$\begin{aligned}
J_n(-x, y) &= (-1)^n J_n(x, y), \\
J_n(x, -y) &= (-1)^n J_{-n}(x, y), \quad (\text{B7}) \\
J_{-n}(x, y) &= J_n(-x, -y).
\end{aligned}$$

Before obtaining the limits of the GBF's for small arguments, it is convenient to write the expansion (B1) in the form

$$\begin{aligned}
J_n(x, y) &= \sum_{l=1}^{\infty} [J_{n-2l}(x) J_l(y) + (-1)^l J_{n+2l}(x) J_l(y)] \\
&\quad + J_n(x) J_0(y). \quad (\text{B8})
\end{aligned}$$

Using the series expansion of the $J_n(\zeta)$ we get the following small argument expansion for $J_n(x, y)$.

(a) n, x fixed and $y \ll 1$. Keeping contributions up to the fourth order in y , we get

$$\begin{aligned}
J_n(x, y)|_{y \ll 1} &\cong \left[J_n(x) + [J_{n-2}(x) - J_{n+2}(x)] \frac{y}{2} \right] \left(1 - \frac{1}{4} y^2 \right) \\
&\quad + [J_{n-4}(x) + J_{n+4}(x)] \frac{y^2}{8}. \quad (\text{B9})
\end{aligned}$$

(b) n, y fixed and $x \ll 1$. Keeping contributions up to the second order in x , we end up with

$$J_n(x, y) \cong \begin{cases} J_{n/2}(y) + \left[\frac{x}{2} \right]^2 [J_{n/2-1}(y) - J_{n/2}(y)] & \text{for } n \text{ even} \\ J_1(x)[J_{(n-1)/2}(y) - J_{(n+1)/2}(y)] + J_3(x)[J_{(n+3)/2}(y) - J_{(n+3)/2}(y)] & \text{for } n \text{ odd} . \end{cases} \tag{B10}$$

Together with $J_n(x, y)$ the modified GBF of the first kind can be defined as

$$I_n(x, y) = \sum_{l=-\infty}^{+\infty} I_{n-2l}(x) I_l(y) , \tag{B11}$$

and their recurrence relations are given by

$$\begin{aligned} \frac{\partial}{\partial x} I_n(x, y) &= \frac{1}{2} [I_{n-1}(x, y) + I_{n+1}(x, y)] , \\ \frac{\partial}{\partial y} I_n(x, y) &= \frac{1}{2} [I_{n-2}(x, y) + I_{n+2}(x, y)] , \end{aligned} \tag{B12}$$

$$2nI_n(x, y) = x [I_{n-1}(x, y) - I_{n+1}(x, y)] + 2y [I_{n-2}(x, y) - I_{n+2}(x, y)] ,$$

and the relevant generating function is

$$\sum_{n=-\infty}^{+\infty} t^n I_n(x, y) = \exp \left[\frac{x}{2} \left(t + \frac{1}{t} \right) + \frac{y}{2} \left(t^2 + \frac{1}{t^2} \right) \right] , \quad |t| < \infty \tag{B13}$$

and

$$\sum_{n=-\infty}^{+\infty} e^{in\theta} I_n(x, y) = \exp [x \cos(\theta) + y \cos(2\theta)] . \tag{B14}$$

In Sec. III we have defined functions of the type

$$\mathcal{D}_n(x, y; z, u) = \sum_{l=-\infty}^{+\infty} I_{n-1}(x, y) J_l(z, u) . \tag{B15}$$

It is also easy to state the relevant recurrence relations, namely,

$$\begin{aligned} \frac{\partial}{\partial x} \mathcal{D}_n(x, y; z, u) &= \frac{1}{2} [\mathcal{D}_{n-1}(x, y; z, u) + \mathcal{D}_{n+1}(x, y; z, u)] , & \frac{\partial}{\partial y} \mathcal{D}_n(x, y; z, u) &= \frac{1}{2} [\mathcal{D}_{n-2}(x, y; z, u) + \mathcal{D}_{n+2}(x, y; z, u)] , \\ \frac{\partial}{\partial z} \mathcal{D}_n(x, y; z, u) &= \frac{1}{2} [\mathcal{D}_{n-1}(x, y; z, u) - \mathcal{D}_{n+1}(x, y; z, u)] , & \frac{\partial}{\partial u} \mathcal{D}_n(x, y; z, u) &= \frac{1}{2} [\mathcal{D}_{n-2}(x, y; z, u) - \mathcal{D}_{n+2}(x, y; z, u)] , \\ 2n\mathcal{D}_n(x, y; z, u) &= x [\mathcal{D}_{n-1}(x, y; z, u) - \mathcal{D}_{n+1}(x, y; z, u)] + 2y [\mathcal{D}_{n-2}(x, y; z, u) - \mathcal{D}_{n+2}(x, y; z, u)] \\ &+ z [\mathcal{D}_{n-1}(x, y; z, u) + \mathcal{D}_{n+1}(x, y; z, u)] + 2u [\mathcal{D}_{n-2}(x, y; z, u) + \mathcal{D}_{n+2}(x, y; z, u)] ; \end{aligned} \tag{B16}$$

and it is also easy, in spite of the apparent complexity, to derive the Jacobi-Anger expansion in the form

$$\sum_{n=-\infty}^{+\infty} e^{in\theta} \mathcal{D}_n(x, y; z, u) = \exp \{ x \cos(\theta) + y \cos(2\theta) + i [z \sin(\theta) + u \sin(2\theta)] \} . \tag{B17}$$

We must, however, quote the possibility of using a generalized Graf theorem to sum (B15) and express $\mathcal{D}_n(x, y; z, u)$ in terms of a single GBF of the $J_n(X, Y)$ type. We will not report the explicit expression that will be discussed elsewhere.

Before closing this appendix we want to underline the possibility of defining a multivariable (> 2), one-index GBF that can be exploited in multipolar scattering prob-

lems. In particular we introduce the GBF

$$J_n(x, y, z) = \sum_{l=-\infty}^{+\infty} J_{n-3l}(x, y) J_l(z) , \tag{B18}$$

whose recurrence properties are just provided by

$$\begin{aligned} \frac{\partial}{\partial x} J_n(x, y, z) &= \frac{1}{2} [J_{n-1}(x, y, z) - J_{n+1}(x, y, z)] , \\ \frac{\partial}{\partial y} J_n(x, y, z) &= \frac{1}{2} [J_{n-2}(x, y, z) - J_{n+2}(x, y, z)] , \\ \frac{\partial}{\partial z} J_n(x, y, z) &= \frac{1}{2} [J_{n-3}(x, y, z) - J_{n+3}(x, y, z)] , \\ 2nJ_n(x, y, z) &= x [J_{n-1}(x, y, z) + J_{n+1}(x, y, z)] \\ &+ 2y [J_{n-2}(x, y, z) + J_{n+2}(x, y, z)] \\ &+ 3z [J_{n-3}(x, y, z) + J_{n+3}(x, y, z)] . \end{aligned} \tag{B19}$$

The relevant Jacobi-Anger expansion reads

$$\sum_{n=-\infty}^{+\infty} e^{in\theta} J_n(x, y, z) = \exp\{i[x \sin(\theta) + y \sin(2\theta) + z \sin(3\theta)]\} \quad (\text{B20})$$

and therefore the relevance of such functions to the problem of the type discussed in this paper is self-evident.

We must emphasize that the GBF provided in the analysis of the undulator brightness is a significant analytical help. The use of double, triple, . . . , infinite series, using conventional Bessel functions only, might create noticeable computational troubles. On the other hand, the properties of the GBF's have allowed the construction of fast and reliable numerical codes, as discussed in Ref. [4], which have also significantly improved the numerical analysis.

-
- [1] H. Winick and S. Doniach, *Synchrotron Radiation Research* (Plenum, New York, 1980).
- [2] R. Barbini, F. Ciocci, G. Dattoli, and L. Giannessi, *Riv. Nuovo Cimento* **6**, 1990.
- [3] D. F. Alferov, Yu. A. Bashmakov, and E. G. Bessanov, *Proc. P. N. Lebedev Phys. Inst. [Acad. Sci. USSR]* **80**, 97 (1976); B. M. Kincaid, *J. Appl. Phys.* **48**, 2684 (1977); W. B. Colson, *IEEE J. Quantum Electron.* **QE-17**, 1417 (1981).
- [4] G. Dattoli, A. Torre, S. Lorenzutta, G. Maino, and C. Chiccoli, *Nuovo Cimento B* **106**, 21 (1991).
- [5] J. D. Jackson, *Classical Electrodynamics* (Wiley, New York, 1975), p. 677.
- [6] G. Dattoli and A. Renieri, in *Laser Handbook*, 4th ed., edited by M. L. Stich and M. S. Bass (North-Holland, Amsterdam, 1985); W. B. Colson, in *ibid.*, 6th ed., edited by W. B. Colson, C. Pellegrini, and A. Renieri (North-Holland, Amsterdam, 1990).